EXTENDING THE SERVICE LIFE OF BRIDGES USING CONTINUOUS DECKS

Adel El-Safty, Ph.D., P.E., Assistant Professor, Dept. of Civil Engineering, University of North Florida, Jacksonville, FL
Ayman M. Okeil, Ph.D., P.E., Assistant Professor, Dept. of Civil and Environmental Engineering, Louisiana State Univ., Baton Rouge, LA

ABSTRACT

The national bridge inventory reveals that our bridges face a persistent performance and maintenance problem. One of the major problems is deck joints that often lead to deterioration in their vicinity. Using jointless bridge decks reduces direct and indirect costs associated with bridge maintenance and repair. This paper presents two approaches to investigate the behavior of jointless bridge deck systems. The first is a detailed nonlinear finite element analysis of bridges subjected to instantaneous, temperature and time-dependent effects that is used as a proof of concept, which was validated using published experimental testing results. Key parameters such as support configurations, time-dependent effects, link slab stiffness, debonded length, and level of reinforcement are investigated. Analytical results of mode of failure, deflections, and strains are presented. A simplified method that is more suitable for design purposes is presented and then used to investigate the instantaneous effects of introducing a link slab to six typical reinforced and prestressed concrete bridges. The study suggested that the use of debonded link slab can be effective in extending the service life of new or repaired bridge deck systems.

Keywords: Jointless, Bridge, Deck, Time-dependent effects, Temperature, Strength

INTRODUCTION

Bridge joints are used to accommodate deck thermal movements and other short and long-term movements caused by creep, shrinkage, moisture changes, vehicular traffic, etc. [1,2]. However, deck joints are costly to buy, install, and maintain. Deck drainage water, contaminated with chemicals like deicing salts, leaks through joints' openings thus damaging the superstructure and the pier caps below and destroying vital bridge parts, such as prestressing cable anchorage systems, beams, bearings. Moreover, the accumulated debris may restrain deck expansion causing increased pavement pressures that squeeze bridge decks [2,3,4]. In addition, there is a high risk of span separation for multi-simple span bridges due to earthquakes or flood & water surge during hurricanes. A good solution is to eliminate the joints using a continuous deck over multiple simple spans. It promotes reduced initial and maintenance costs, improved riding quality, lower impact loads, and improved seismic resistance. The construction of a fully-continuous jointless bridge deck with partial debonding from the ends of simple girders (such as shown in Fig. 1) provides a simple and economic solution not only for the construction of new bridges but also for the maintenance and rehabilitation of old ones, by re-decking the existing simply supported girders [3,5-9]. The link slab connecting and bridging the gap between the two adjacent simple span girders with partial debonding of the deck from the girders ends at supports is investigated.

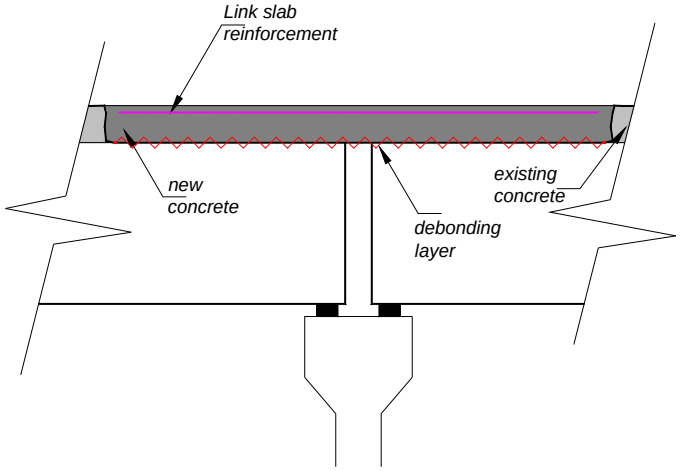

Fig. 1: Link slab with partial debonding at girder ends.

Several methods for the analysis of jointless deck systems were proposed [3,4,9]. The load-deflection response of a jointless bridge deck was investigated using a finite element method[4] modeling the divided bridge span into a number of isoparametric beam elements, with the link slab as a spring element having only axial stiffness. A simplified design procedure was proposed based on elastic analysis for partially debonded and continuous decks indicating the effect of support conditions on stresses and potential cracking in the deck. Later, a modified finite element program was developed and its results showed that the optimum debonded length is between 2% and 6% of the girder span depending on the conditions of support and loading [3,7]. Also, a test program was initiated for two bridge models of 2 simply supported beams composite with the deck that is debonded at beam ends for a length of 5% of each girder span[8]. Subsequently, a design concept for the link slab based on the previous test program and analytical studies was presented [7,8]. The bridge was considered as simply-supported since the flexural stiffness of link

slab was relatively very small compared to that of the girders and since the debonding of link slab for 5% of girder spans would not alter the load-deflection behavior of jointless bridge decks[8]. It was also assumed that the link slab was subjected to flexure rather than axial deformation and cracks occurred at the midpoint. If the moment in the link slab exceeded the cracking moment, the moment of inertia of the cracked section was used at the middle part of the slab and the effective moment of inertia for the debonded portion was computed [8]. Recently, partial continuity due to the axial stiffness of link slab and support configurations was investigated [1] using a modified three-moment equation. Repair of the Story Bridge in Australia was reported by eliminating contraction joints[5]. A re-decking case study where joints were eliminated was reported[10]. The construction of a demonstration bridge with jointless decks in North Carolina, U.S., was reported. The positive performance of jointless bridge decks in seismic zones is demonstrated [11]. Long-term effects were also investigated by several researchers [12].

A repair work was done for the southern approach to the Story Bridge crossing the Brisbane River in Australia[5]. Thirty six deteriorated contraction joints (approximately spaced at 20.3 ft.) were removed and the deck slab was made continuous over every five spans but the simply supported steel stringers that were composite with the slab remained discontinuous. The deck was partially debonded from the girder ends.

In this study, the concept of joint-free decks is first investigated using numerical analysis that accounts for linear and nonlinear, instantaneous and time-dependent responses, and strength of simply supported girders, partially debonded from a continuous deck. The analysis is based on the finite element method which is capable of analyzing both composite and non-composite, fully continuous and non-continuous girders, and system of simple girders supporting continuous deck, having different steel reinforcement ratios, under different loading and support conditions. The effects of dead and live loads, prestressing, temperature variations, and time-dependent effects of aging, creep, shrinkage and relaxation are considered. The model is then validated by comparing the results of analysis with available analytical and experimental results. Finally, the modified three-moment equation that was developed by Okeil and ElSafty [1] is utilized to estimate the reduction in live load moments due to the introduction of link slabs. Finally, the impact of this positive moment reduction on fatigue life is quantified for reinforced and prestressed concrete girder bridges.

DETAILED ANALYSIS OF BRIDGES WITH CONTINUOUS JOINT-FREE DECKS

Investigations of the behavior of a bridge composed of a deck stiffened by eccentric girders were conducted [3, 4], considering composite action except at debonded portions. For the finite element analysis, an iso-parametric beam element (Fig. 2-a) is used for the analysis of girders and a spring like element is used for modeling the reinforced concrete link slab “connection element” and is located at the deck centroid away from the composite section centroid and having only axial stiffness. The flexural stiffness of the deck is neglected at the connection element; however, a rotational restriction is provided by the spring due to its offset position from the centroid of the composite section. Iso-parametric beam elements have the property of coordinate transformation and displacement field through the same (ISO) set of interpolation functions, commonly known as shape functions. Prestressing forces are accounted for by specifying initial prestressing strains in the tendons before releasing of the tendon forces. The strains can be determined from the

stress level and the instantaneous stress-strain relationship of the tendon steel. The tendon forces vary continually with time and along the length of the tendon after transfer of the prestressing forces. The tendon profiles are represented by their centroidal lines and may be approximated as straight segments within the element length. The tendon forces were taken as constant within each element. The relations between displacements at the element nodal points and displacements at the extremities of the tendon are shown in Fig. 2-b. The prestressing force variation due to friction is shown in Fig. 2-c. The tendon stiffness matrix was included into the beam element stiffness matrix when analyzing pre-tensioned girders. However, for post-tensioned girders, the tendon stiffness matrix was superimposed after performing the analysis first to obtain the effects of initial prestressing.

Beam spans are divided into isoparametric beam elements and each element is further divided into layers for the girders and the deck. Both instantaneous and time-dependent responses as well as linear and nonlinear ranges of behavior of beams are implemented. An incremental method, to solve for displacements, is performed using the tangent stiffness matrix of the system, either by increments of load or displacement. For girders subjected to prestressing or its own dead load and deck dead load, analysis is performed by using the Load Increment Method. However, after the composite action is established, the girders are analyzed by using the Displacement Increment Method for an increasing concentrated live load up to failure. With the continuous deck providing a negative moment connection at support piers, the bridge behaves as a partially continuous structure for loads applied after casting the deck. The degree of continuity depends on time-dependent material behavior, loading and support condition. Bearing supports are modeled as uniaxial spring-like elements attached to the respective nodal points. H stands for a hinged support and R for a roller support (bearing with free horizontal movement).

TIME-DEPENDENT RESPONSE ANALYSIS

The behavior of composite bridge girders may vary, when subjected to loading at different ages, due to the non-linear time-dependent material properties, such as in creep, shrinkage, aging of concrete, and relaxation of prestressing steel. In performing time-dependent response analysis, the time interval may be divided into several small increments. Within such small time increments, the instantaneous solution is used. In each time increment or step, material properties and the response of each layer of the beam follow the time-functions and stress level history up to the start of the time increment. The equilibrium position of the member is used as the basis for the response analysis in the following time step. The time of applying loads is also considered in a similar manner. Loads and restraints are applied at nodal points. Strains in each layer consist of time-dependent strain parts in addition to instantaneous strain parts. Shrinkage strain is a function of time alone thus can be found immediately at any given time increment. Under variable stresses, two methods for predicting creep strains may be used. The two methods are the Rate of Creep Method and the Superposition Method. Relaxation strains are treated the same way as creep strains and stresses are calculated from the stress history using a method similar to the rate of creep method. The time-dependent strains at any incremental time-step, are related to stresses and transformed into nodal forces. Then, the load vector is applied to the model and an age-corrected instantaneous solution is performed, seeking the current equilibrium position of the member. This process is repeatedly applied for each increment of time until the time-dependent response of the member is obtained.

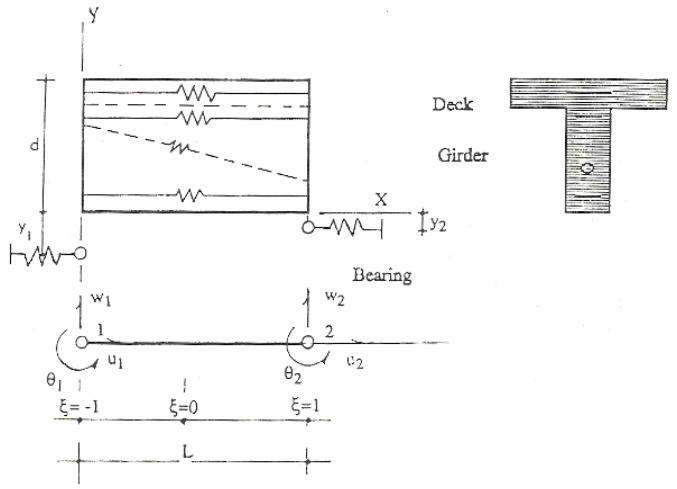

(a) Element components and degrees of freedom

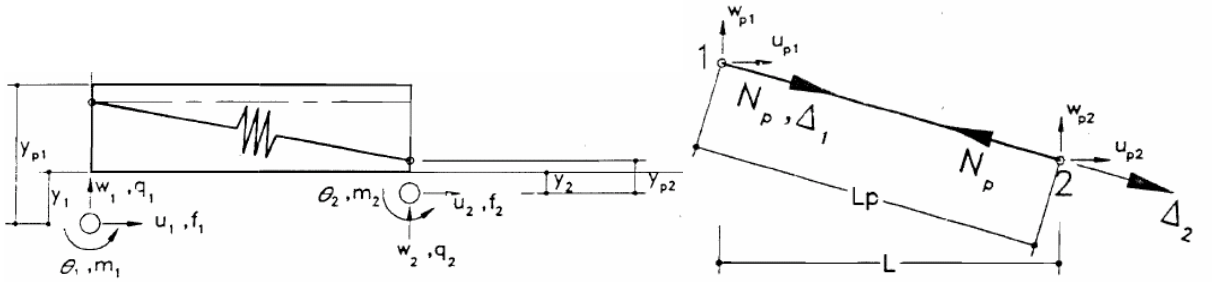

(b) Prestressing Cable Model within the Beam Element

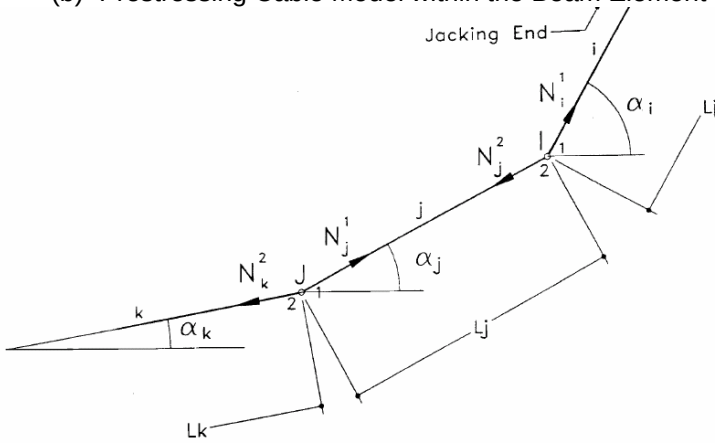

(c) Prestressing force variation due to friction

Fig. 2: Details of Isoparametric Beam Element

Bridges are also subjected to temperature variations due to seasonal changes and daily cycles that vary with time. Thermal effects are analyzed considering a given temperature distribution over the composite cross-section, as it is non-variable along the member length and stationary in time. A Bi-linear variation was used as an approximation to the non-linear temperature gradient. The inclusion of temperature effects in the finite element solution is performed by treating the thermal strains ε_T as initial strains ε_o. Thermal strains $\varepsilon_T = \alpha \Delta T$, while α is the coefficient of thermal expansion and ΔT is the temperature-change that may induce thermal strains ε_T when

free deformation is restrained. The initial strain vector $\{\varepsilon_o\}$ is introduced to the beam element and the final stresses may be written as $\{\sigma\} = [E]\{\varepsilon - \varepsilon_o\}$, where ε is the current strain vector exclusive of the effects of $\{\varepsilon_o\}$. The nodal forces vector $\{f\}$ is:

$$\{f\} = \int_v [B]^T \{\sigma\} dv \tag{1}$$

Substituting $\{\sigma\}$ into the previous equation yields to:

$$\{f\} = \int_v [B]^T [E]\{\varepsilon\} dv - \int_v [B]^T [E]\{\varepsilon_o\} dv \tag{2}$$

which can be expressed in terms of nodal forces vector $\{f_o\} = \int_v [B]^T [E]\{\varepsilon_o\} dv$ that is caused by the effect of specified initial strains $\{\varepsilon_o\}$ on the element

$$\{f\} = [K]\{\Delta\} - \{f_o\} \tag{3}$$

By rearranging Equation 3

$$\{f\} + \{f_o\} = [K]\{\Delta\} \tag{4}$$

VALIDATION OF THE ANALYTICAL MODEL WITH EXPERIMENTAL TESTING

The results from an experimental program [8, 9] were used to validate the proposed analytical model. Results of test specimen (Fig. 3) are compared in Table 1. The results of midspan deflection and link slab rebar stress are reported [3, 8] under an applied load of 15 kips. The support conditions for one half of the structure are as follows: Case 1- all rollers, Case 2- roller-hinge-roller-hinge, Case 3- roller-hinge-hinge-roller, and Case 4- hinge-roller-roller-hinge. A fixed support is assumed at the line of symmetry. In case of RHHR supports, there is a significant discrepancy of the deflection test results with the analytical model. That might be attributed to the possibility of support movements that would prevent the development of a large continuity moment between the girders in the case of RHHR

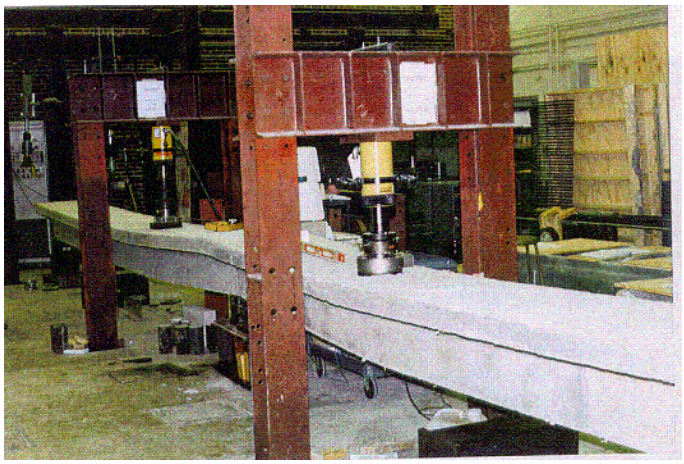

Fig. 3: Experimental Testing of Jointless Bridge

Table 1: Comparison of Concrete Bridge Test Results with FEM Program Results

Case	Results	East Mid Span Deflection (in.)	West Mid Span Deflection (in.)	Link Slab Rebar Stress (ksi)
HRRH	Test	0.21	0.21	12.5
	FEM program	0.16	0.16	-1.40
RHRH	Test	0.22	0.22	12.3
	FEM program	0.17	0.28	7.2
RHHR	Test	0.21	0.21	12.2
	FEM program	0.04	0.04	28.2

EFFECT OF SUPPORT CONDITIONS ON GIRDER BEHAVIOR

The load-deflection responses for the composite girder, under different support arrangements, are shown in Fig. 4. Comparison is made with the extreme cases of a fully-continuous girder and a non-continuous girder that represent the upper and lower bounds, respectively. The beam in support case (RHHR) having two intermediate hinges, develops higher ultimate load than the beams in other cases of all-roller supports and (RHRH). Higher stiffness in the linear range is reported for beams with supports (RHHR) and (RHRH) than that of beams with all-roller supports and with HRRH. Failure of the beam in Case 1, with roller supports, is due to crushing of concrete at top fiber of mid span where the ultimate compressive strain is reached. The beam in Case 2 fails due to yielding (with a strain of 0.01) of steel reinforcement in the connection element. However, the beam in Case 3 fails due to yielding of steel reinforcement in the connection element. For beam with Case 4, compressive force is developed in the first connection element and a tension force in the second one.

EFFECT OF DEBOND ON JOINTLESS DECK

The effect of partially debonding the deck from girders ends was investigated under different support conditions. For four-span prestressed concrete beams with equal loading in Case 3 (RHHR), Fig. 5 shows the improvement in the load carrying capacity with partial debond of the concrete deck from the girder ends. The optimum ultimate load was obtained for the beam with a

debonded length of 0.05 of the girder span. The ultimate load carrying capacity, with a debonded length of 0.05 L, was higher than the beam without debond by about 11.5%. A more ductile behavior was also achieved with the debonded beams (Fig. 5). Other beams with debonded lengths of 0.02 L up to 0.08 L also showed comparable improvement in the load carrying capacity. If the deflection is restricted, the debonded length may be limited to a value within the range of 0.02 L to 0.05 L.

Moreover, the debonded beam exhibited much more ductility. For the linear response, beams with different debonded lengths showed similar stiffness within the service load range. For yield of the deck reinforcement, all beams exhibited yielding of the deck steel and concrete cracking in the connection element. The force increase in the deck connection of the debonded beams was virtually linear before yielding of the deck reinforcement. Then, a constant force was maintained until failure. It was observed that under service load conditions, the steel stresses remained in the elastic range, thus enabling cracks to close upon unloading of the structure.

Failure of all the beams was due to yielding (with a maximum strain of 0.01) of the steel reinforcement in the deck connection element.

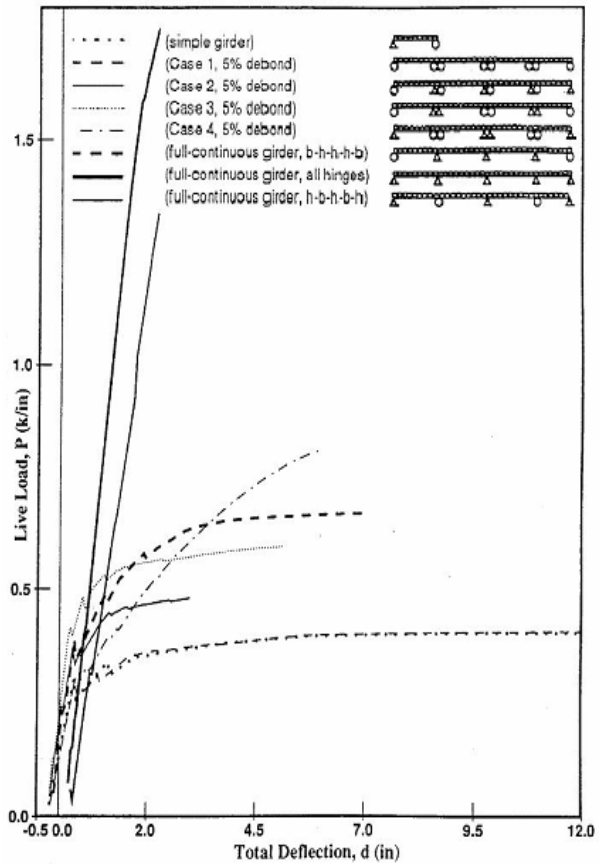

Fig. 4: Load-deflection responses for prestressed concrete beams with 5% debond, different supports cases

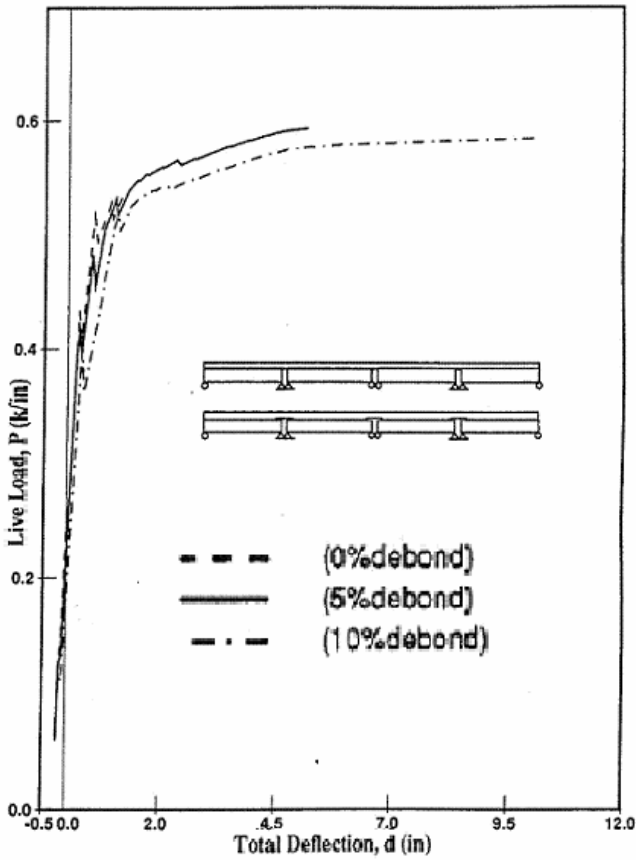

Fig. 5: Effect of 5% debond on load-deflection response for beams) with supports Case 3

EFFECT OF REINFORCEMENT RATIO ON LOAD-DEFLECTION RESPONSE

Beams with different deck reinforcement at the connection element were investigated under equal loading. For the beams with case-3 support condition and with/without debonded length, Fig. 6 shows an increase in the ultimate load of the beams by increasing the steel content in the connection element. The steel reinforcement ratios are 0.5%, 0.75%, 1%, 1.56%, 2%, 2.6%, 3%, 4%, 5%, and 6% of the cross-sectional area of the concrete deck. It was observed that the beam response comes closer and closer to the response of the full continuous beam. The failure occurs mainly due to yielding (with a strain of 0.01) of the reinforcing steel in the connection element. However, for reinforcement ratios of 3% and more (for beams without debond) and 6% and more (for debonded beams), the steel in the connection element may yield but does not reach the prescribed strain of 0.01 before the beam fails near its mid span due to crushing of concrete.

TIME-DEPENDENT AND TEMPERATURE EFFECTS

For debond effect on beams under creep, beams were analyzed successively for girder dead load, deck dead load, prestressing, and live load. The creep effect was included in each of the first three loadings. Beams with debonded lengths ranging from 0.01 to 0.10 of the span length, were analyzed. Fig. 7 shows an increase in the load-carrying capacity for the debonded beams than the beams without debond with the highest load carrying capacity at a debonded length of 0.05 L. Its ultimate load is higher than that of unbonded beam by about 11.6%. Its failure is due to yield (with a strain of 0.01) of steel reinforcement in the connection element. A more ductile behavior is also noticed for debonded beams.

For effect of aging, shrinkage and creep of concrete and steel relaxation, deck-continuous beams with or without debonded length were analyzed for their responses under time-effects. The beams were left unloaded for a period of one year under the effects of aging, shrinkage and creep of concrete and relaxation of the prestressing steel. Afterwards, the beams were loaded to failure. No perceptible difference between time-dependent and instantaneous strengths, of beams with and without debond, was found as the results of the time dependent effects. However, debonded beams showed a higher ultimate load and a more ductile response than the beams without debond.

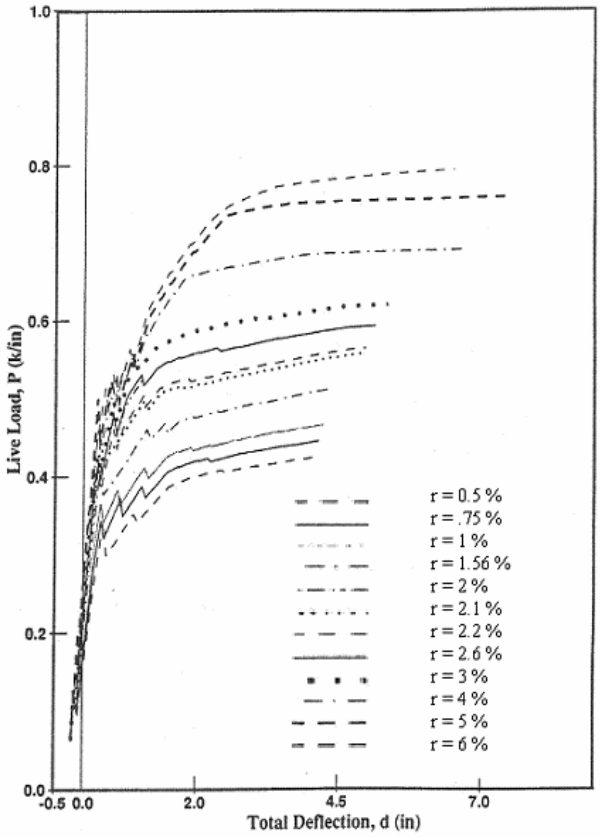

Fig. 6: Effect of deck steel ratio on load-deflection response for beams (4 spans with 5% debond - supports case 3

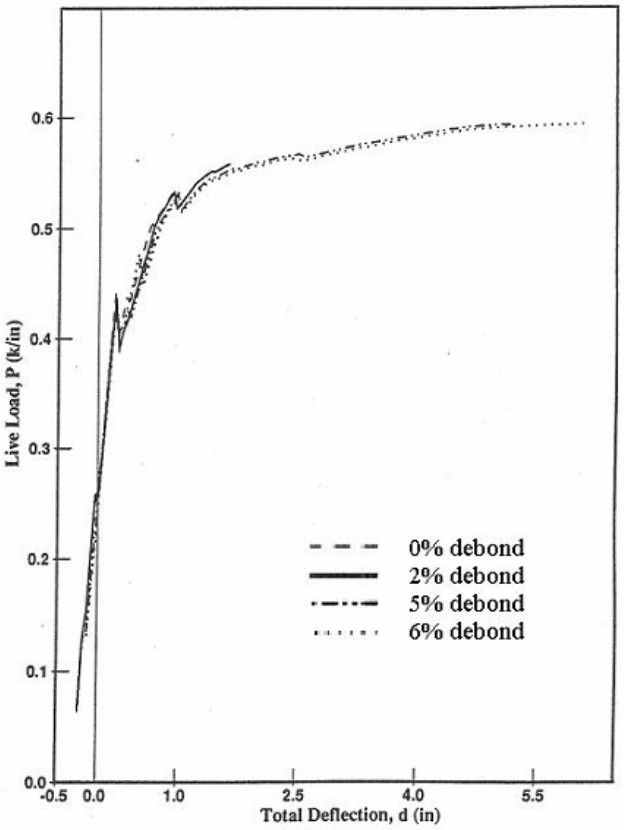

Fig. 7: Effect of debond on prestressed beams under creep (4 spans-support case 3)

For temperature effect, beams with and without debond were analyzed for their responses under temperature effects (Fig. 8). Both beams were supported with rollers and loaded with equal loading. No perceptible difference was found in beams responses under the effect of a temperature gradient. It was seen that camber increases when temperature varied across the depth of the beams. However, under a constant temperature gradient, very slight changes in deflection were observed.

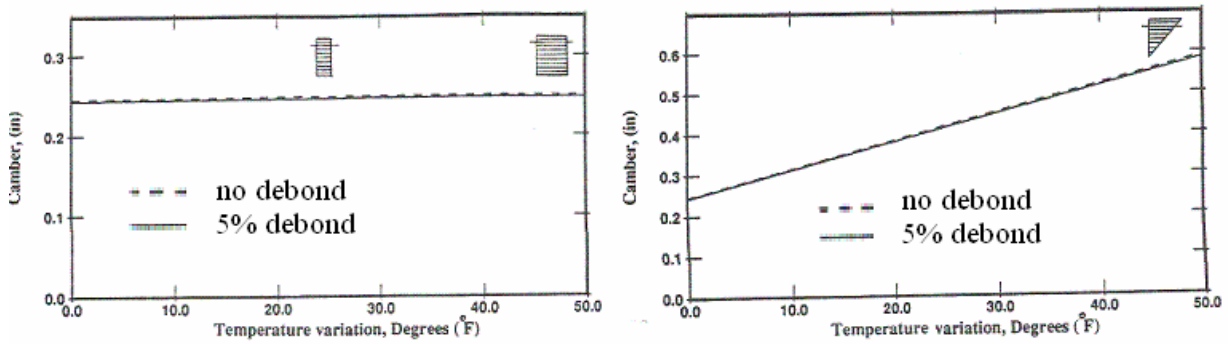

Fig. 8: Debond effect on beams under temperature variations (4-spans, rollers supports)

SIMPLIFIED ANALYSIS OF BRIDGE GIRDERS WITH CONTINUOUS JOINT-FREE DECKS

A simplified analysis procedure for bridges with jointless decks was developed by Okeil and ElSafty[1]. The procedure is an extension of the classic *Three Moment Equation* that is known to be very efficient for continuous beam analysis. The classical form of the equation is given as

$$M_0 \frac{L_{\mathrm{L}}}{(EI)_{\mathrm{L}}} + 2M_1\left[\frac{L_{\mathrm{L}}}{(EI)_{\mathrm{L}}} + \frac{L_{\mathrm{R}}}{(EI)_{\mathrm{R}}}\right] + M_2 \frac{L_{\mathrm{R}}}{(EI)_{\mathrm{R}}} = -6\left[\frac{r_{1\mathrm{L}}}{(EI)_{\mathrm{L}}} + \frac{r_{1\mathrm{R}}}{(EI)_{\mathrm{R}}}\right] \tag{5}$$

where M_i=continuity moments at the supports; r_{1L} and r_{1R}=central support reactions due to the elastic load, M/EI, by considering each span independently; and EI and L are, respectively, the flexural rigidity and span length.

In deriving Equation 5, it is assumed that the compatibility between girder end rotations at the supports is fully maintained. This assumption is plausible for fully continuous girders. However, jointless decks do not enforce this compatibility condition. Okeil and ElSafty[1] used link slab extension as a new compatibility condition. The link slab extension was link to girder end rotations at the support under consideration, $\alpha_{1\mathrm{L}}$ and $\alpha_{1\mathrm{R}}$, which leads to the following expression for the RHHR configuration

$$-\alpha_{1\mathrm{L}} h + \alpha_{1\mathrm{R}} h = \frac{T}{k_{link}} = \frac{\left[-\frac{M_1}{h}\right]}{k_{link}} \tag{6}$$

where h=distance from the support to the deck centroid (Fig. 9); T=tension force; and k_{link}=axial stiffness of the link slab. Assuming the link slab is fully cracked, k_{link} can be replaced by its axial stiffness, $E_s A_s / L_{\mathrm{link}}$, where A_s =area of steel provided in the link slab, E_s=modulus of elasticity for steel, and L_{link}=length of the link slab reinforcement including any debonded length[8]. The modified three-moment equation for the RHHR configuration was then obtained by substituting for variables in Equation 5 from Equation 6 and rearranging:

$$M_0 \frac{L_{\mathrm{L}}}{E_g I_{g\mathrm{L}}} + 2M_1\left[\frac{L_{\mathrm{L}}}{E_g I_{g\mathrm{L}}} + \frac{L_{\mathrm{R}}}{E_g I_{g\mathrm{R}}} + 3\frac{L_{link}}{h^2 E_s A_s}\right] + M_2 \frac{L_{\mathrm{R}}}{E_g I_{g\mathrm{R}}} = -6\left[\frac{r_{1\mathrm{L}}}{E_g I_{g\mathrm{L}}} + \frac{r_{1\mathrm{R}}}{E_g I_{g\mathrm{R}}}\right] \tag{7}$$

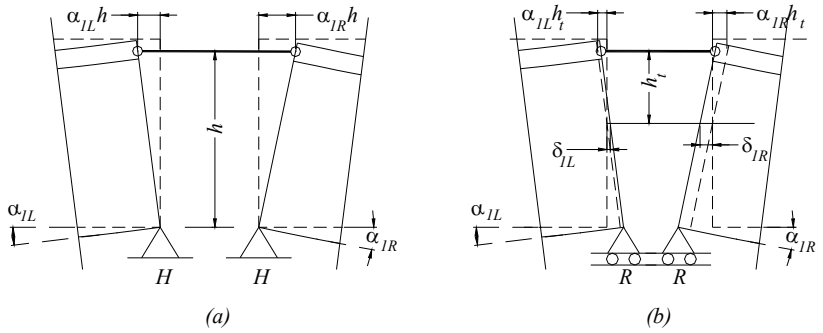

Fig. 9: Support movement in a jointless system (a) hinged support configuration (RHHR) and (b) roller support configuration (HRRH)

Similarly, the link slab extension for the HRRH case can be written. In this case, the elongation of the girders, δ_{1R} and δ_{1L} due to the tension force resisted by the far support leads to the following expression:

$$\left(-\alpha_{1\mathrm{L}}h_t-\delta_{1\mathrm{L}}\right)+\left(\alpha_{1\mathrm{R}}h_t-\delta_{1\mathrm{R}}\right)=\frac{T}{k_{link}} \tag{8}$$

which leads to the following modified three-moment equation for HRRH case is

$$\begin{aligned} M_0\frac{L_{\mathrm{L}}}{E_gI_{g\mathrm{L}}}+2M_1\left[\frac{L_{\mathrm{L}}}{E_gI_{g\mathrm{L}}}+\frac{L_{\mathrm{R}}}{E_gI_{g\mathrm{R}}}+\frac{3}{h_t^2}\left(\frac{L_{\mathrm{L}}}{E_gA_{g\mathrm{L}}}+\frac{L_{\mathrm{R}}}{E_gA_{g\mathrm{R}}}+\frac{L_{link}}{E_sA_s}\right)\right] \\ +M_2\frac{L_{\mathrm{R}}}{E_gI_{g\mathrm{R}}}=-6\left[\frac{r_{1\mathrm{L}}}{E_gI_{g\mathrm{L}}}+\frac{r_{1\mathrm{R}}}{E_gI_{g\mathrm{R}}}\right] \end{aligned} \tag{9}$$

PARTIAL CONTINUITY MOMENT IN A TWO-SPAN BRIDGE

In the case of a two-span girder bridge, the end moments, M_0 and M_2, are equal to zero because of end conditions. As a result, Equations 7 reduces to the following expression in the case of RHHR support configuration:

$$2M_1\left[\frac{L_{\mathrm{L}}}{E_gI_{g\mathrm{L}}}+\frac{L_{\mathrm{R}}}{E_gI_{g\mathrm{R}}}+3\frac{L_{link}}{h^2E_sA_s}\right]=-6\left[\frac{r_{1\mathrm{L}}}{E_gI_{g\mathrm{L}}}+\frac{r_{1\mathrm{R}}}{E_gI_{g\mathrm{R}}}\right] \tag{10}$$

and the following expression for HRRH support configurations:

$$2M_1\left[\frac{L_{\mathrm{L}}}{E_gI_{g\mathrm{L}}}+\frac{L_{\mathrm{R}}}{E_gI_{g\mathrm{R}}}+\frac{3}{h_t^2}\left(\frac{L_{\mathrm{L}}}{E_gA_{g\mathrm{L}}}+\frac{L_{\mathrm{R}}}{E_gA_{g\mathrm{R}}}+\frac{L_{link}}{E_sA_s}\right)\right]=-6\left[\frac{r_{1\mathrm{L}}}{E_gI_{g\mathrm{L}}}+\frac{r_{1\mathrm{R}}}{E_gI_{g\mathrm{R}}}\right] \tag{11}$$

These expressions can then be used to obtain special influence lines (I.L.) for continuity moments at the support under consideration. For a generic unit load located at a distance x from the left support, it is possible to write the solution for the continuity moment, M_1, in terms of the ratio between unit load location and span length, $\alpha = x/L_{\mathrm{L}}$. The continuity moment, M_1, at the inner support for the RHHR configuration is

$$M_{1,RHHR} = \frac{-\frac{1}{2}\alpha\left(1-\alpha^2\right)L_{\mathrm{L}}^2}{\left[L_{\mathrm{L}} + L_{\mathrm{R}} + 3\frac{L_{link}}{h^2}\frac{E_g I_g}{E_s A_s}\right]} = -\frac{1}{2}\frac{\alpha\left(1-\alpha^2\right)L_{\mathrm{L}}}{\left[1+\beta+3\psi\right]} \tag{12}$$

where, $\beta = L_{\mathrm{R}}/L_{\mathrm{L}}$ is the span length ratio and, $\psi = \frac{L_{link}}{L_{\mathrm{L}}h^2}\frac{E_g I_g}{E_s A_s}$ is a link slab stiffness coefficient. In deriving Equation 12, it is assumed that both spans have the same cross-sectional and material properties; i.e., $I_{g\mathrm{L}}=I_{g\mathrm{R}}=I_g$ and $A_{g\mathrm{L}}=A_{g\mathrm{R}}=A_g$., for simplicity.

Similarly, the following expression was derived for the continuity moment in HRRH configuration

$$M_{1,HRRH} = -\frac{1}{2}\frac{\alpha\left(1-\alpha^2\right)L_{\mathrm{L}}}{\left[1+\beta+3\left\{\left(1+\beta\right)\lambda+\frac{\psi}{\gamma^2}\right\}\right]} \tag{13}$$

in which β and ψ are as before, γ is a shape factor equal to h_t/h, and λ is a variable which accounts for the axial deformation of the girders, $\lambda = \frac{I_g}{h_t^2 A_g}$. Fig. 10 shows the influence lines for the continuity moment and the positive moment for a two equal-span bridge. For comparison purposes, the influence lines for the case of a fully continuous girder and a simply supported girder are also plotted. It can be seen that the case of roller supports (HRRH) introduces little continuity compared to the hinged support case (RHHR).

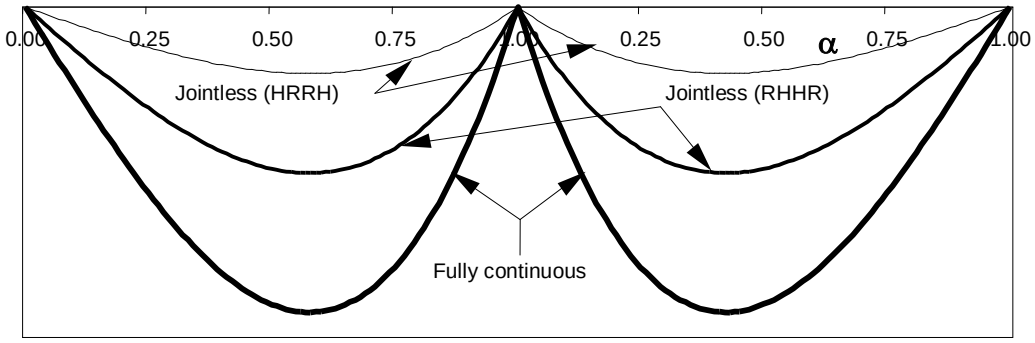

(a)

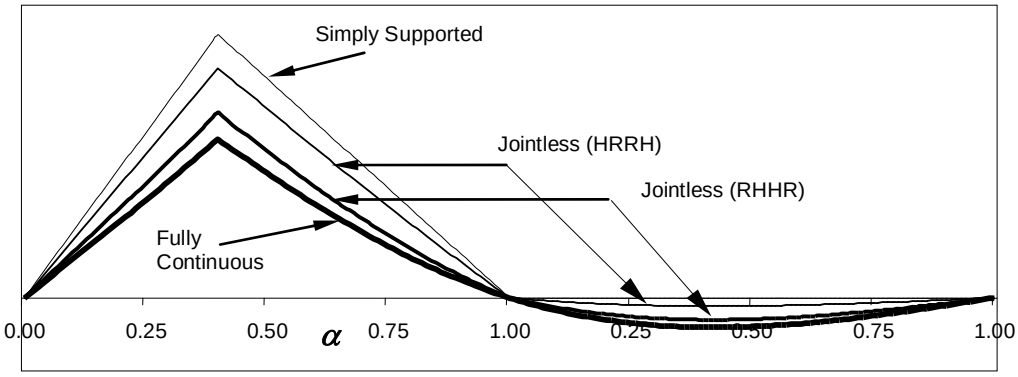

(b)

Fig. 10: Influence Line of a Two-Span Bridge (a) Continuity Moment (b) Positive Moment at α =0.4

IMPACT OF PARTIAL CONTINUITY ON FATIGUE LIFE

As has been demonstrated by previous work, jointless decks introduce partial continuity in girder bridge superstructures. The introduction of continuity leads to the development of negative moments when live loads are applied, which in turn reduce the positive moments in comparison with simply supported girder bridge superstructures. In this section of the paper, the impact of this positive moment reduction on fatigue life will be quantified for reinforced and prestressed concrete girder bridges.

SAMPLE RC AND PS GIRDER BRIDGES

Six bridges will be used to demonstrate the impact of introducing partial continuity by means of a jointless deck. Three are assumed to be simply-supported reinforced concrete T-girder bridges, while the other three represent prestressed concrete AASHTO girder bridges. The bridges have the cross sections shown in Fig. 11. Three span lengths were considered for RC bridges (45 ft, 60 ft, and 75 ft) and three span lengths for PS bridges (60 ft, 80 ft, and 100 ft). The link slab reinforcement was assumed to be 1% of the area of the slab.

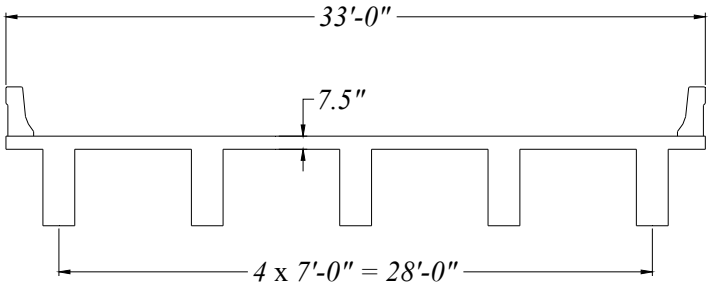

(a) RC Bridges

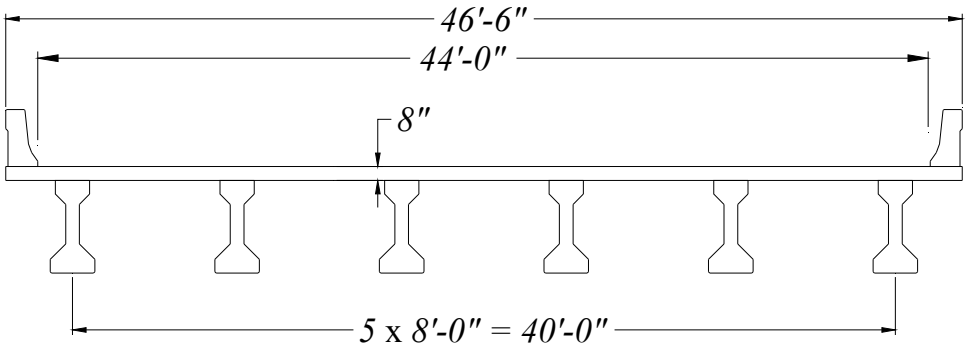

(b) PS Bridges

Fig. 11: Cross-sectional dimensions of sample bridges

Based on the geometric and material properties of the bridges, the jointless parameters β, ψ, λ, and γ were computed and are listed in Table 2.

Table 2: Properties of Sample Bridges

Bridge	L (ft)	Section	f_c' (psi)	β	ψ	λ	γ
RC45	45	16.0in x 39.0in	4000	1.0	0.1338	1.767	0.246
RC60	60	18.0in x 51.0in			0.1742	1.256	0.299
RC75	75	22.0in x 63.5in			0.2298	0.908	0.351
PS60	60	Type II	7000		0.1237	2.244	0.233
PS80	80	Type III			0.1612	1.614	0.287
PS100	100	Type IV			0.2004	1.266	0.329

ESTIMATES OF REDUCTION IN POSITIVE MOMENT

For a typical positive moment load case, HL-93 loading [15] would have to be positioned as seen in Fig. 12.

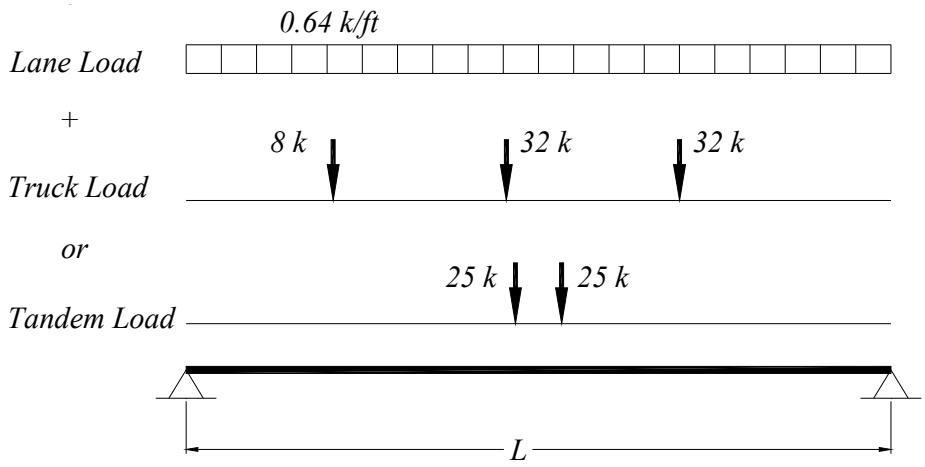

Fig. 12: HL-93 loading on simply supported bridge

Using the expressions in Equations 7 and 9, the live load continuity moment caused by the introduction of the link slab was first computed for the same loading position. At the critical section for positive moment, only one-half of the partial continuity moment impacts the maximum positive moment values. The positive live load moment was computed at mid spans for the HRRH and RHHR cases, respectively. The computed moment values are listed in Table 3. Also listed in the table are the live load moment values for the simply supported case and the dead load moment.

Table 3: Dead and Live Load Moments in Girders (k.ft.)

Bridge	M_D	M_L				
		Simple	HRRH		RHHR	
			Magnitude	Diff.	Magnitude	Diff.
RC45	343	611	587	-3.9%	484	-20.8%
RC60	741	951	902	-5.2%	763	-19.8%
RC75	1487	1373	1283	-6.6%	1118	-18.6%
PS60	661	925	896	-3.2%	730	-21.1%
PS80	1334	1385	1327	-4.2%	1107	-20.1%
PS100	2383	1906	1807	-5.2%	1540	-19.2%

LL STRESS RANGE IN BRIDGES WITH JOINTLESS DECKS

Table 3 shows that the reduction in live load moments is in the range of 4.7% for HRRH support configurations and 19.9% for RHHR support configurations. This reduction in LL moments is directly proportional to the LL stress level in girder reinforcement since fatigue stresses are estimated under service conditions; i.e. materials are still within their elastic limit. As a result, it can be said that the introduction of link slabs will also reduce LL stresses in reinforcing bars or strands. According to AASHTO-LRFD [13], the cyclic stress range in the reinforcement should be checked for the *Fatigue* limit state, which would clearly benefit from the reduction caused by the introduction of the link slab. It should be noted that unlike the simply supported case where the

minimum LL stress is equal to zero, the minimum LL stress for partially continuous girders is compression as a result of loading the adjacent span with live loads. Quantifying the extension in design life is possible using results reported herein. However, it is an involved procedure and requires detailed information about the specifics of the reinforcement material, especially its *S-N* curves.

CONCLUSIONS

The following conclusions are drawn concerning the flexural behavior of jointless bridge deck and girder systems with partially debonded connections.

- The simply supported girders supporting fully continuous deck with partial debonding from the girders ends (optimum debonded length of 0.05 of the beam span) is a good alternative for reducing deck joint maintenance.
- Introducing link slabs in typical bridges may reduce the live load stress range between 4.7% and 19.9%. This would positively impact the fatigue life of the girders, which may be quantified if required material and traffic information is available.
- The tension force that develops in the link slab is affected by the system's support configuration. The boundary conditions greatly affect the responses and stiffness of the jointless deck and girder system.
- Increasing the steel content in the connection element will enhance the girder response and its ultimate load to approach the response of continuous girder. Yet, increasing the reinforcement in the connection element beyond a certain limit may result in the failure of deck due to crushing of concrete.
- Under creep effects associated with both dead loads and prestressing, an increase in the load carrying capacity and ductility are observed for debonded girders in comparison with girders without debond.
- Camber increases when temperature varies across the depth of the beams. However, under a constant temperature gradient, very slight, rather negligible, changes in deflection are observed

LIST OF NOTATIONS

α	coefficient of thermal expansion
ΔT	temperature change
$\{\varepsilon\}$, $\{\varepsilon_o\}$, $\{\varepsilon_T\}$	strain, initial strain, thermal strain vectors in FE analysis
$\{\sigma\}$	stress vector in FE analysis
$\{f\}$, $\{f_o\}$	force, initial force vectors in FE analysis
$\{K\}$	element stiffness matrix in FE analysis
$\{d\}$	displacement vector in FE analysis
$[E]$	stress-strain (constitutive) matrix in FE analysis
$[B]$	strain-displacement (compatibility) matrix in FE analysis
EI	flexural rigidity of girder

h	total girder height
k_{link}	axial stiffness of link slab
L_L, L_R, L_{link}	length of right span, left span and link slab
M_o, M_1, M_2	continuity moments in two-span segment of a continuous beam
r_{1L}, r_{1R}	reactions due to elastic loads at support under consideration
β	span length ratio
ψ	link slab stiffness coefficient
γ	shape factor
λ	axial deformation coefficient

REFERENCES

[1] Okeil, A.M. and El-Safty, A.K. “Partial Continuity in Bridge Girders with Jointless Decks,” Practice Periodical on Structural Design and Construction, ASCE, Nov. 2005, pp 229-238.

[2] Burke, M.P., "Flawed assumptions: Why bridge deck joints fail", Civil Engineering, Nov. 1991, pp. 60-62.

[3] El-Safty, A.K., “Behavior of Jointless Bridge Decks “, North Carolina State University, Ph.D. Dissertation, May 1994.

[4] Gastal, Francisco P.S.L., "Instantaneous and time-dependent response and strength of jointless bridge beams", NCSU, Ph.D, 1987.

[5] Demartini, C. J., and Heywood, R. J., "Repair of the Southern Approach to the Story Bridge by Elimination of the Contraction Joints", Austroads Conference Brisbane, Australia, 1991, pp. 357-370.

[6] Richardson, D. R, "Simplified Design Procedures for the Removal of Expansion Joints from Bridges Using Partially Debonded, Continuous Decks", Master's Thesis, North Carolina State University, 1989.

[7] Zia, P. Caner, A., and El-Safty, A.K., “Jointless Bridge Decks”, Technical, FHWA/NC/95-006, North Carolina Department of Transportation, Report, Sept. 1995.

[8] Caner, A. and Zia, P., Behavior and design A of link slabs for jointless bridge decks”, PCI Journal, May-June 1998, pp 68-80.

[9] Thippeswamy, H. K., GangaRao, H. V. S., and Franco, J. M., “Performance evaluation of jointless bridges” *Journal of Bridge Engineering*, ASCE, 7(5), 2002, pp. 276–289.

[10] Pierce, P. (1991). “Jointless redecking”, *Civil Engineering*, 61(9), 1991, pp. 60–61.

[11] Caner, A., Dogan, E., and Zia, P., “Seismic performance of multisimple-span bridges retrofitted with link slabs.” *Journal of Bridge Engineering*, ASCE, 7(2), 2002, pp. 85–93.

[12] Siros, K. A., and Spyrakos, C. C., “Creep analysis of hybrid integral bridges.” *Transportation Research Record*, *1476*, Transportation Research Board, Washington, D.C., 1995, pp. 147–154.

[13] AASHTO, *LRFD Bridge Design Specifications*, American Association of State Highway and Transportation Officials, Washington, D.C., 2004.